Composites Science and Technology 70 (2010) 2128–2136

Contents lists available at ScienceDirect

Composites Science and Technology

journal homepage: www.elsevier.com/locate/compscitech

Compression-after-impact response of woven fiber-reinforced composites

Hao Yan, Caglar Oskay *, Arun Krishnan, Luoyu Roy Xu

Department of Civil and Environmental Engineering, Vanderbilt University, Nashville, TN 37235, USA

ARTICLE INFO

Article history:
Received 12 April 2010
Received in revised form 23 July 2010
Accepted 17 August 2010
Available online 24 August 2010

Keywords:
B. Delamination
C. Multiscale modeling
C. Damage mechanics
C. Finite element analysis
Compression-after-impact

ABSTRACT

This manuscript investigates compression-after-impact failure in woven fiber-reinforced composites. Compression failure of composite structures previously damaged by an impact event is due to the propagation of impact-induced damage mechanisms such as interlaminar debonding, constituent (i.e., matrix and fiber) microcracking, sublaminate buckling, as well as the interactions between these mechanisms. The failure mechanisms within each ply are idealized based on a reduced order multiscale computational model, in which, the damage propagation in the matrix and fibers upon compression is explicitly modeled. Delamination along the ply interfaces is idealized using a cohesive surface model. The initial impact-induced damage within the microconstituents and interfaces are inferred from experimental observations. A suite of numerical simulations is conducted to understand the sublaminate buckling, propagation of delamination and constituent damage upon compression loading. The numerical investigations suggest extensive propagation of delamination with mode transition preceding sublaminate buckling. Initiation and propagation of matrix and fiber cracking, observed upon sublaminate buckling, is the cause of ultimate shear failure.

1. Introduction

Fiber-reinforced composites have been gaining prominence as high performance structural materials in aerospace, naval and automotive industries due to their high specific strength and stiffness. One of the main difficulties with fiber-reinforced composite structures is that their performance degrades once subjected to impact of even modest magnitudes. It is well known that the compressive strength reduces after an impact event, such as tool drop, runway debris impact, bird strikes, and ballistic projectiles in the case of aerospace structures. The impact event typically causes matrix cracking, fiber breakage and delamination within the structure. Under compressive loads, these failure mechanisms interact and the impact-induced damage propagates to failure at significantly lower load levels compared to the undamaged state [1,2].

Considerable research has been devoted to the experimental analysis of compression-after-impact (CAI) behavior of fiber-reinforced composites (e.g., [3–9] among many others). The main foci of the experimental investigations have been (1) characterization of damage within the material due to impact and (2) phenomenological correlation of the reduction in the compressive strength to the impact-induced damage. The primary triggering mechanism of failure in impacted composites is the buckling of sublaminates formed due to the impact event [10]. Impact-induced delamination occurs at a roughly circular region around the impact site. The delaminated region cause local buckling of the sublaminates under compressive loads. The size of the delaminated zone increases with the energy of the impact event, reducing the CAI strength of the material [5,8,9,11]. In addition to the sublaminate buckling, CAI strength may be affected by additional impact-induced damage mechanisms including, distinct matrix cracks at the impact surface, matrix and fiber microcracking, as well as weakening of the interlaminar cohesive strength beyond the delamination zones. Systematic studies of the interactive effects of these damage processes have been relatively scarce. The CAI performance of composites is also significantly affected by the microstructural configuration [9], the mechanical properties of the constituent materials, particularly the resin [11], stacking sequence [12,13] and specimen thickness [2,14,7].

A number of analytical approaches have been proposed for the prediction of CAI strength (e.g., [15–18] among others). Chai et al. [15] employed a fracture mechanics criterion to model the stable and unstable delamination growth in laminated composites. Soutis and coworkers [17] observed the similarity between the failure patterns in laminated composites with an open-hole and impact-damaged composites, and employed a fracture toughness model, originally proposed for open-hole geometry, to predict the CAI strength. Xiong et al. [16] proposed a multistep analytical prediction method, in which the impact damage is modeled as an elliptical soft inclusion. In addition to analytical methods a number of numerical investigations have been conducted to predict the

* Corresponding author. Address: VU Station B#351831, 2301 Vanderbilt Place, Nashville, TN 37235, USA.
E-mail address: caglar.oskay@vanderbilt.edu (C. Oskay).

0266-3538/$ - see front matter © 2010 Elsevier Ltd. All rights reserved.
doi:10.1016/j.compscitech.2010.08.012

buckling load and CAI strength (e.g., [19–21], among others). While the prediction strategies have been relatively successful in estimating the CAI strength, devising preventive strategies against strength degradation requires detailed analysis of failure in the pre- and post-buckling loading regimes, in which all dominant failure mechanisms and their interactions are taken into account [22].

In this manuscript, we conduct a detailed numerical analysis of the compression-after-impact response of a woven fiber composite composed of E-glass fibers and vinyl ester resin. Failure mechanisms of matrix cracking and fiber breakage are explicitly modeled based on a multiscale computational method recently proposed by Oskay and coworkers [23,24]. The propagation of impact-induced delamination at multiple ply interfaces is idealized using a cohesive surface model. The impact-induced damage is incorporated by considering the presence of an initial matrix crack, presence of initial delamination with circular geometry between plies, as well as initial damage along the ply interface outside the delaminated zone. Simulations of a composite specimen subjected to compression-after-impact loading is compared to experimental results. The failure progression along the ply interfaces as well as within the composite constituents is analyzed to identify the failure patterns under compressive loading.

2. CAI experiments

Glass fiber-reinforced vinyl ester (glass/VE) panels were produced using vacuum assisted resin transfer molding (VARTM) process [25]. Eight layers of plain weave glass fabric (CWR 2400/50 plain weave, Composites One, LLC) were used to produce the panels with 4.95 ± 0.1 mm thickness as required by ASTM D 7137 specification. The fiber fraction of the panels was found to be 54 vol. percent after burn off testing was conducted. Compression-after-impact (CAI) testing samples with dimensions 101.6 ± 0.1 mm × 152.4 ± 0.1 mm (4″ × 6″ ± 0.004) were cut and machined to meet the strict dimension requirement specified in ASTM D 7137.

Impact damage was introduced using a drop tower setup [26]. All samples were subjected to an impact with 60 J impact energy using a 16 mm (5/8″) diameter hemisphere impactor. Damage zones of the impacted samples are clearly seen in Fig. 1a and c (at the front and back faces). For the front surface directly subjected to impact, light areas represent internal delamination, with possible several delaminations at the different interfaces. Delaminations were nearly circular in shape with largest radius of 17.6 mm ± 1 mm observed between the back plies. A horizontal and a vertical major matrix crack with dimensions 35.8 and 35.1 ± 2 mm, respectively, was observed near the impact site as shown in Fig. 1a. Immediately behind the drop weight impact site, fiber breakage was observed and this failure mode contributed to impact energy absorption (Fig. 1c). Significant kink banding was not observed in the experiments.

Impacted samples were then mounted into the compression fixture and subjected to compression loading based on ASTM D 7137 specification at the rate of 1 mm/min. Strain gages were attached on the sample back and front surfaces to monitor the strain variations at both surfaces during compression. The reason to use strain monitoring is to avoid any global laminate buckling during compression. The progressive compression failure started from the impact damage site as shown in Fig. 1. Initially, as the compression load increased, impact-induced delamination progressively propagates. The final failure was controlled by sudden extension of the horizontal matrix crack toward the edges of the specimen, as shown in Fig. 1b and d, in addition to the formation of a shear crack through the thickness as shown in Fig. 2. The shear crack was inclined at an angle of 30°–45° with respect to the compressive loading direction. No significant kink band formation was observed within the shear failure zone.

3. Numerical modeling of CAI failure

The geometry, discretization, boundary conditions and impact-induced damage considered in the numerical investigations are illustrated in Fig. 3. A 101.6 × 152.4 cm rectangular plate with 5 mm thickness is modeled. The thickness direction displacement is constrained ($u_3 = 0$) along the edges of the front and back side of the plate, as prescribed by the compression-after-impact test fixture. The compression loading is imparted on the specimen by prescribing vertical displacement at the top surface. The bottom surface of the specimen is restrained in the vertical direction. In the numerical simulations, the prescribed vertical displacements are imposed by considering Dirichlet type boundary condition: $u^2 = \tilde{u}(t)$. $\tilde{u}(t)$ is the prescribed displacement history of the boundary, which is taken to be linearly increasing at the top surface of the specimen and homogeneous at the bottom surface of the specimen. The compressive loading of the specimen mimics the loading in the experimental investigations.

3.1. Impact-induced damage

Four mechanisms of impact-induced damage are considered: (1) the presence of a matrix crack along the fill (horizontal)

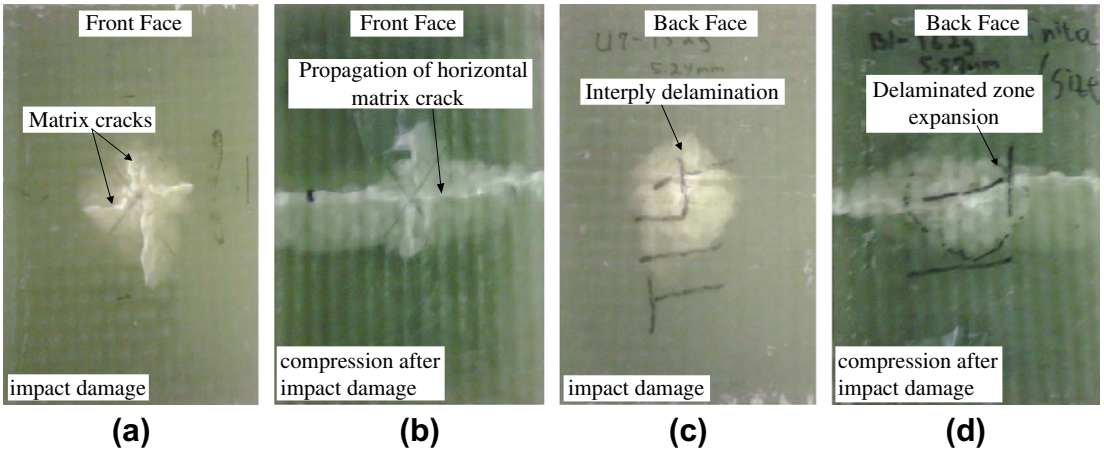

Fig. 1. Damage profiles: (a) impact-induced damage profile viewed from the front (impacted) face, (b) damage profile after compression loading viewed from the front face, (c) Impact-induced damage profile viewed from the back face, and (d) damage profile after compression loading viewed from the back face.